http://app.pan.pl/SOM/app71-Saitta_etal_SOM.pdf

SUPPLEMENTARY ONLINE MATERIAL FOR

Dinosaur “mummification”: Clay templating in a fluvial setting preserves three-dimensional integument renderings after carcass desiccation

Evan T. Saitta, Paul C. Sereno, Daniel Vidal, Maria Ciudad Real, Tyler M. Keillor, Lauren Bop, Stephanie L. Baumgart, Aidan Burdick, Viktor J. Radermacher, Thomas G. Kaye, Laure Dussubieux, Evan Maxey, Alexander S. Filatov, and Xinqi Chen

Published in *Acta Palaeontologica Polonica* 2026 71 (3): 535-579.
https://doi.org/10.4202/app.01349.2026

Supplementary Online Material

Material: Early adult *Edmontosaurus* ‘mummy’ (UCRC PV30); Wyoming, USA, Late Cretaceous.
Late juvenile *Edmontosaurus* ‘mummy’ (UCRC PV31); Wyoming, USA, Late Cretaceous.

SOM 1. Thin Sectioning

A block of tail spikes from the early adult *Edmontosaurus* 'mummy' (UCRC PV30) was stabilized with Epotek 301 and sent to Spectrum Petrographics to produce thin sections. The sectioning locations, as sent to Spectrum Petrographics, are photographed in Figure S1.

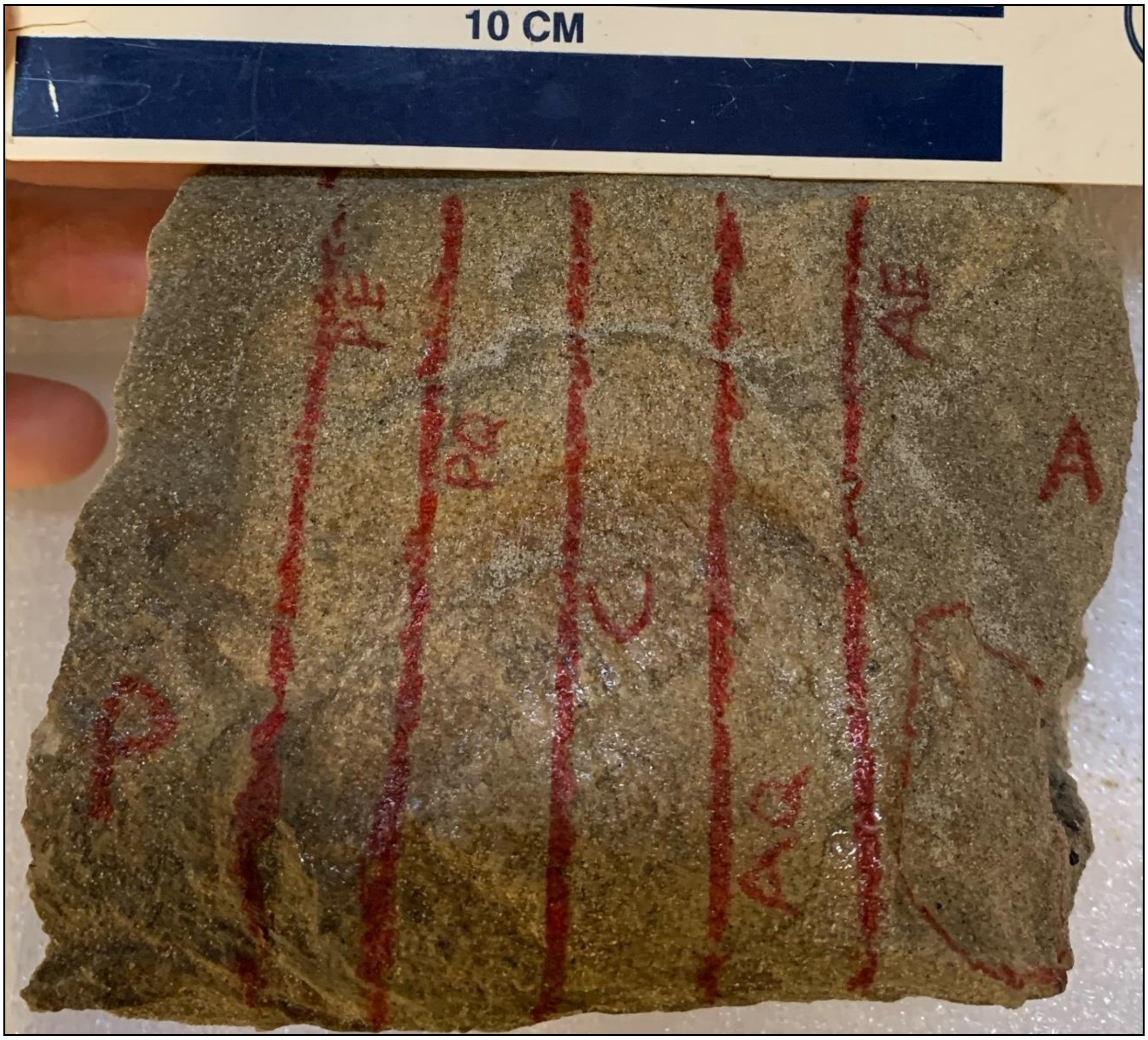

Figure S1. Thin section guide for the adult 'mummy' tail spike block after removal (red marker on epoxy-stabilized surface). A = anterior. P = posterior. Lines indicate sectioning locations. AE = anterior end. AQ = anterior quarter section. C = center. PQ = posterior quarter. PE = posterior end. Circle indicates the manually exposed cross section after removal of the adjacent spike that was fully prepared in three dimensions. Ventral direction is to the bottom of the image. Photograph taken with an iPhone 14.

SOM 2. Light Microscopy

Transverse thin sections from the block of tail spikes (Figure S1) from the early adult *Edmontosaurus* 'mummy' (UCRC PV30) were examined with a Nikon Eclipse LV150N optical microscope at Loyola University (images stitched with Nikon NIS software). Plane polarized and lambda polarized light results shown in Figures S2–S6.

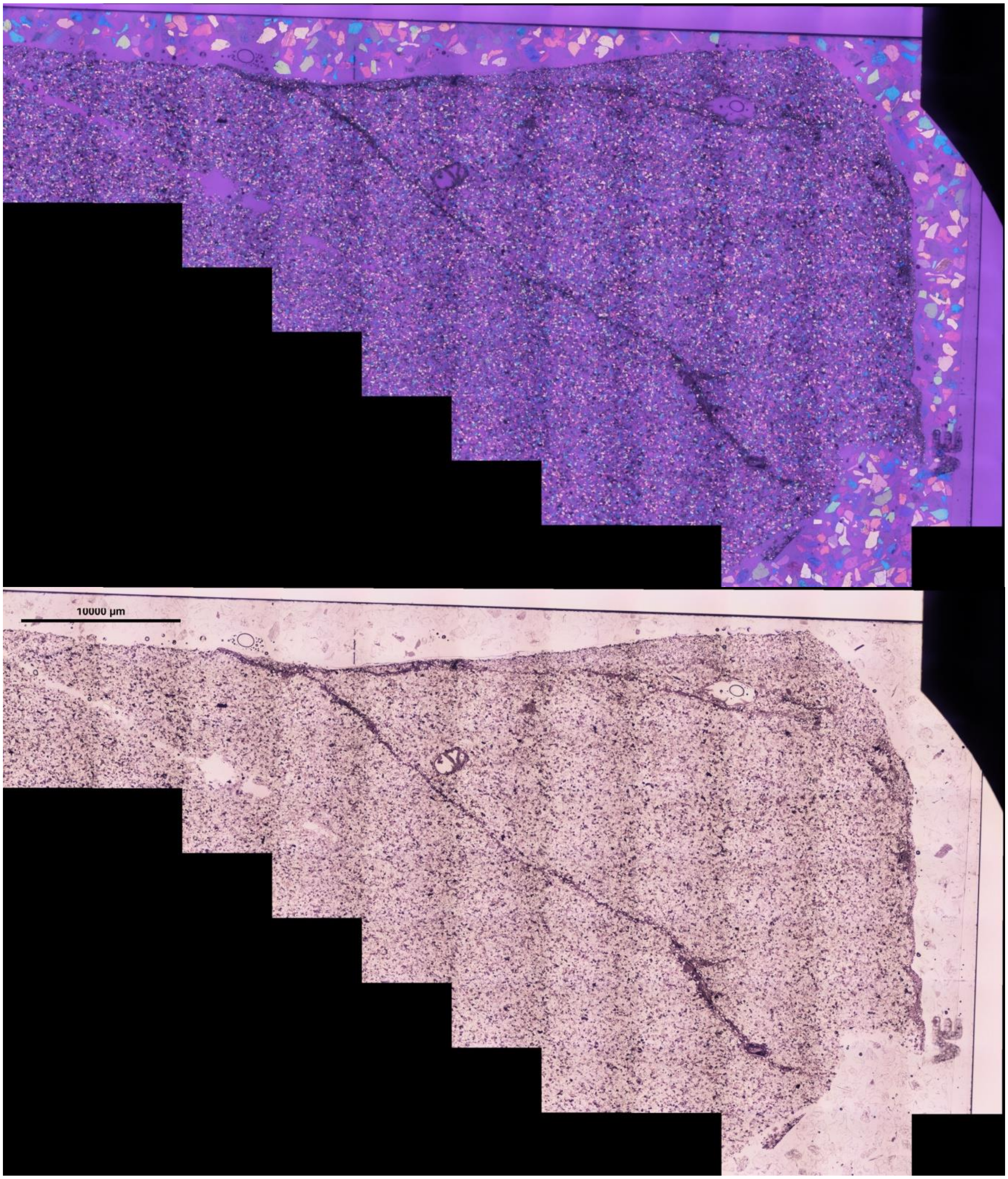

Figure S2. Anterior end (AE) transverse thin section viewed under lambda (top) and plane (bottom) polarized light. Dorsal to left of image.

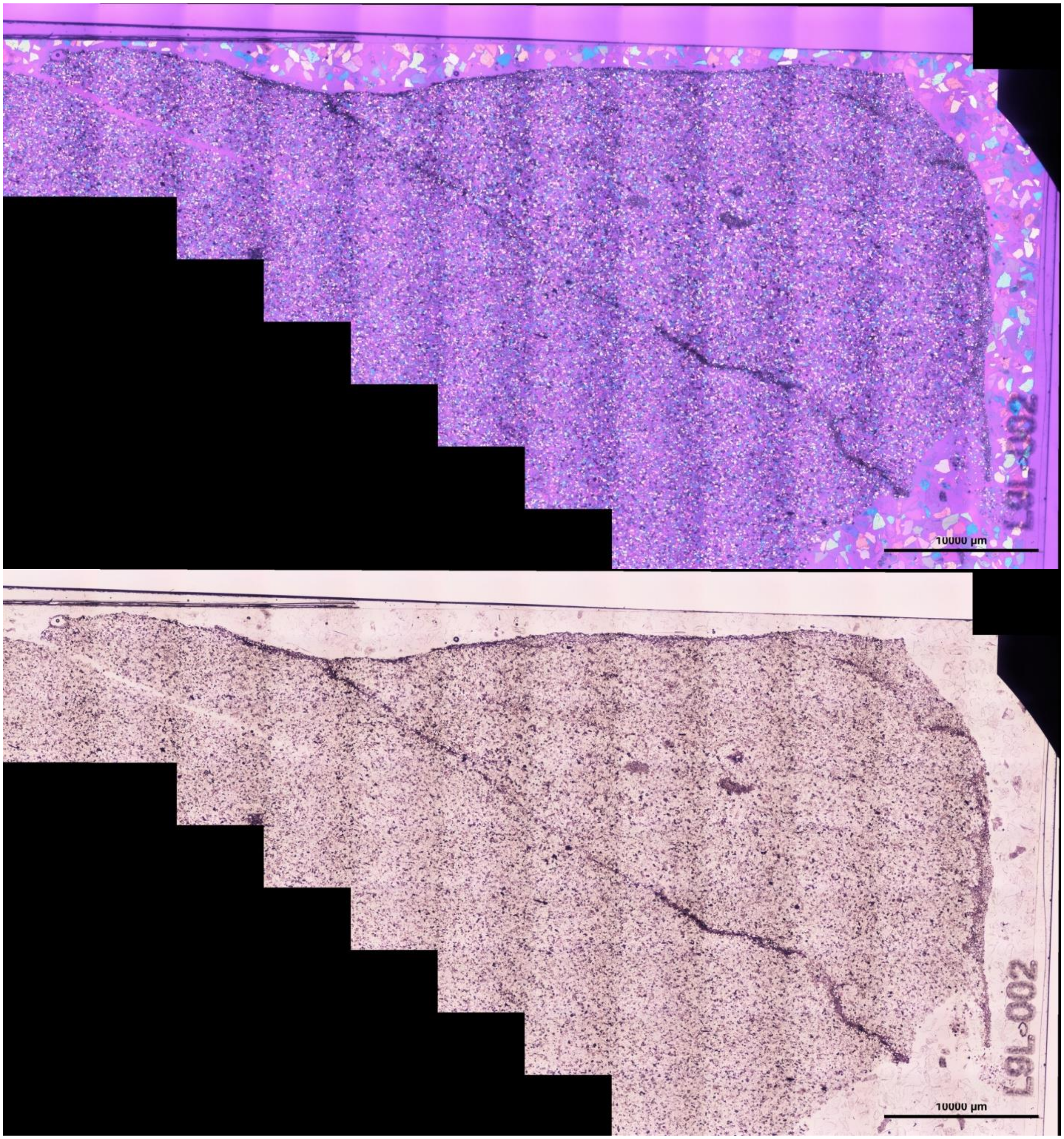

Figure S3. Anterior quarter (AQ) transverse thin section viewed under lambda (top) and plane (bottom) polarized light. Dorsal to left of image.

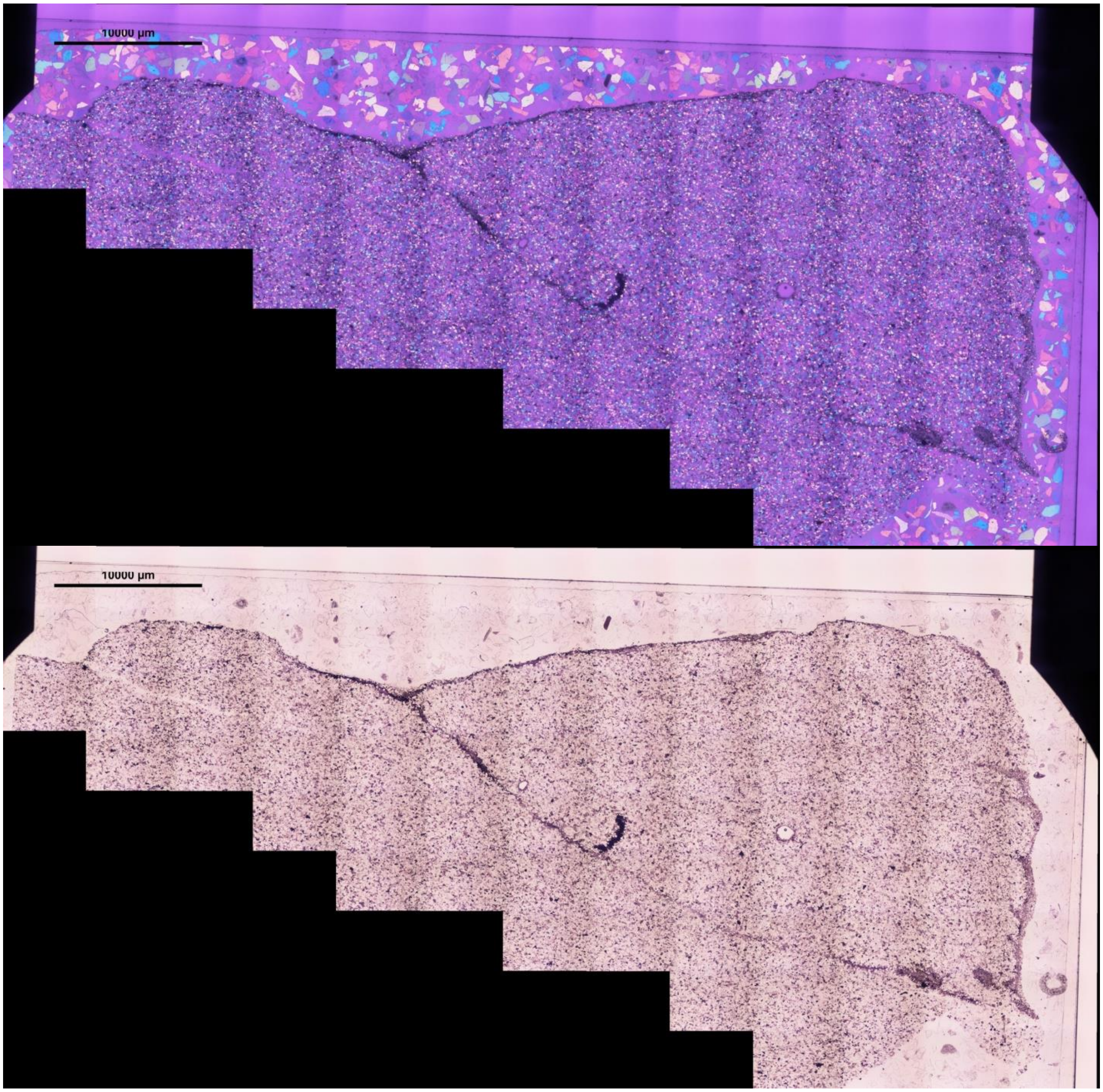

Figure S4. Center (C) transverse thin section viewed under lambda (top) and plane (bottom) polarized light. Dorsal to left of image.

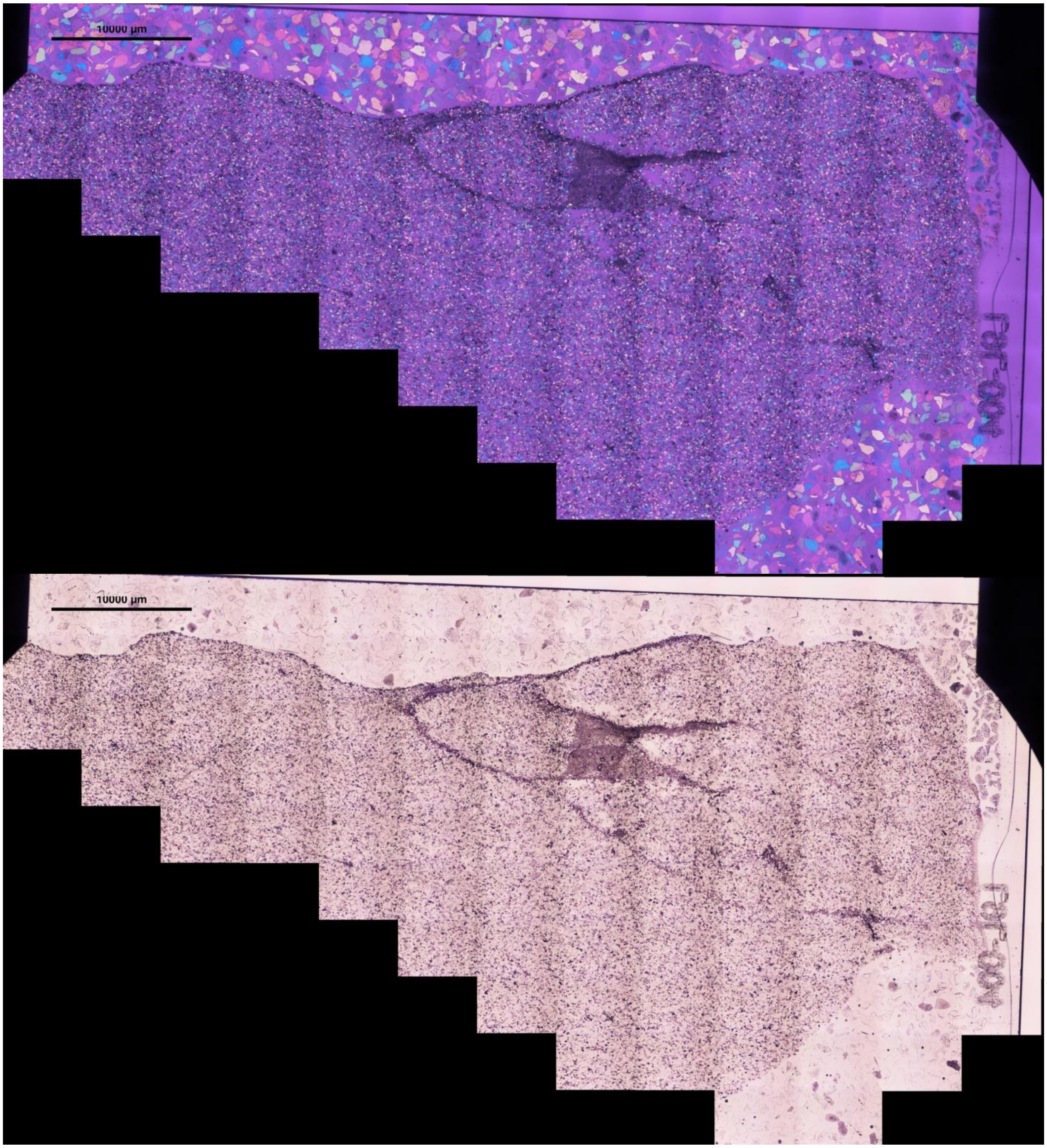

Figure S5. Posterior quarter (PQ) transverse thin section viewed under lambda (top) and plane (bottom) polarized light. Dorsal to left of image.

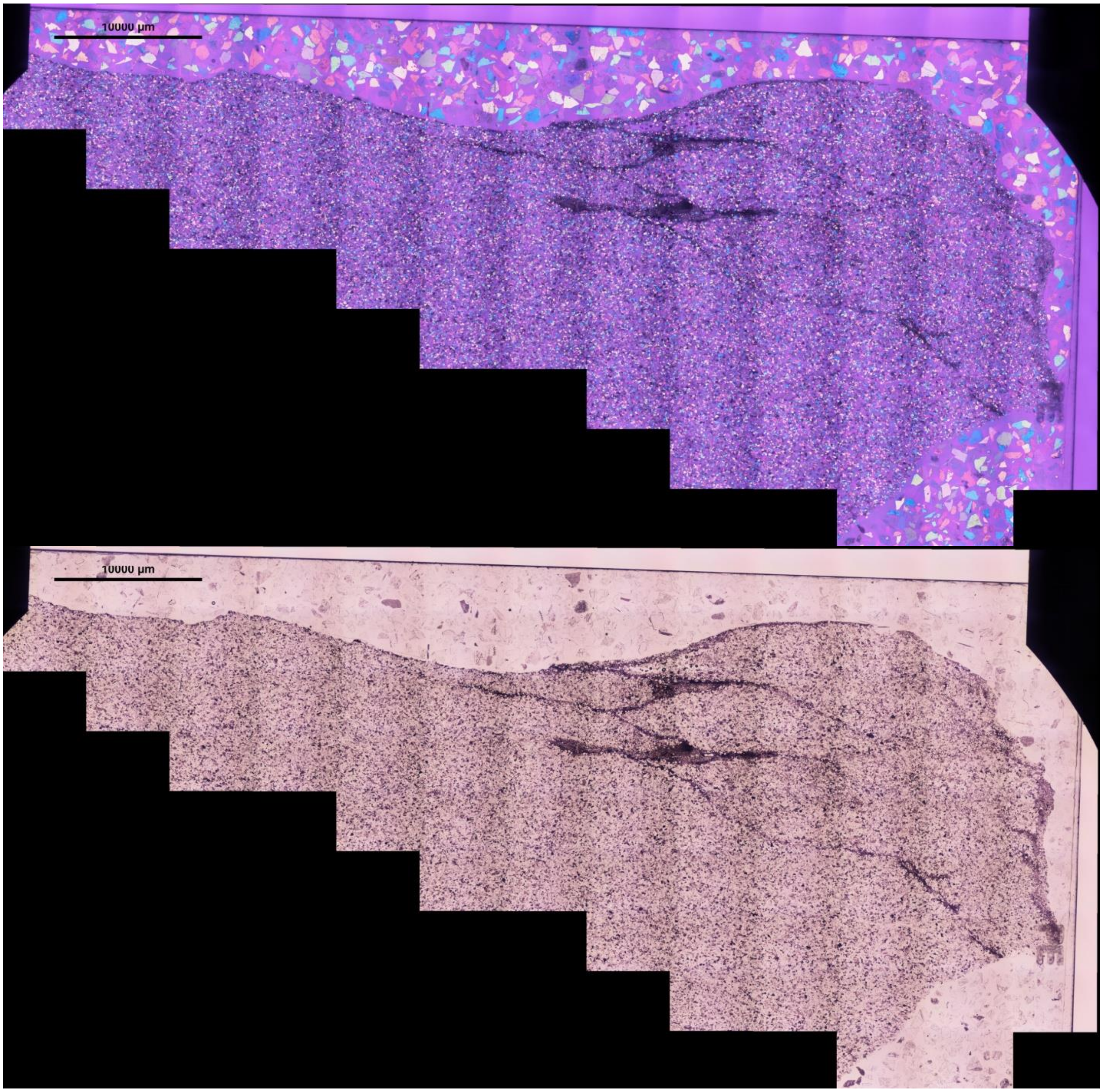

Figure S6. Posterior end (PE) transverse thin section viewed under lambda (top) and plane (bottom) polarized light. Dorsal to left of image.

SOM 3. Synchrotron XRF

A small block of integument rendering separated near the base of the tail on the early adult *Edmontosaurus* ‘mummy’ (UCRC PV30) during excavation, when the jackets were separated for removal. We analyzed this block using synchrotron XRF (see Figure 9 for elemental maps). The raw XRF spectrum is shown in Figure S7.

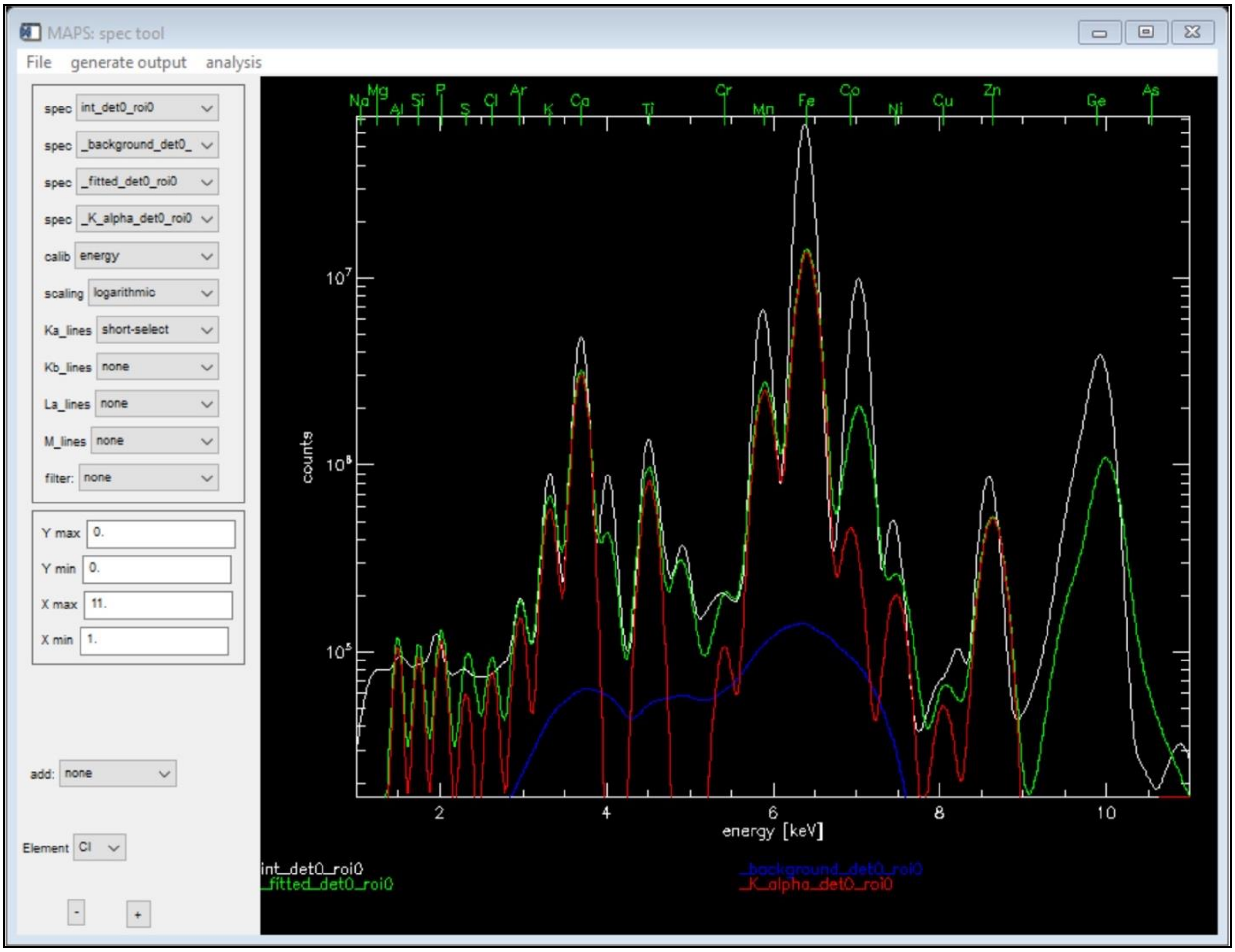

Figure S7. Screenshot of the raw sXRF spectrum of the early adult *Edmontosaurus* ‘mummy’ (UCRC PV30) integument rendering.

SOM 4. Electron Microscopy & Energy Dispersive X-ray Spectroscopy

4.1. Thin section L9L 005 (PE) of the early adult 'mummy' spike (UCRC PV30) –

Averaged EDS spectra were taken from 10 regions of interest (ROI) on thin section L9L 005 from the posterior end (PE) of the early adult *Edmontosaurus* 'mummy' spike (UCRC PV30), with two spectra taken before to calibrate EDS settings (not reported). These regions of interest are indicated on the BSE image of the spike thin section in Figure S8.

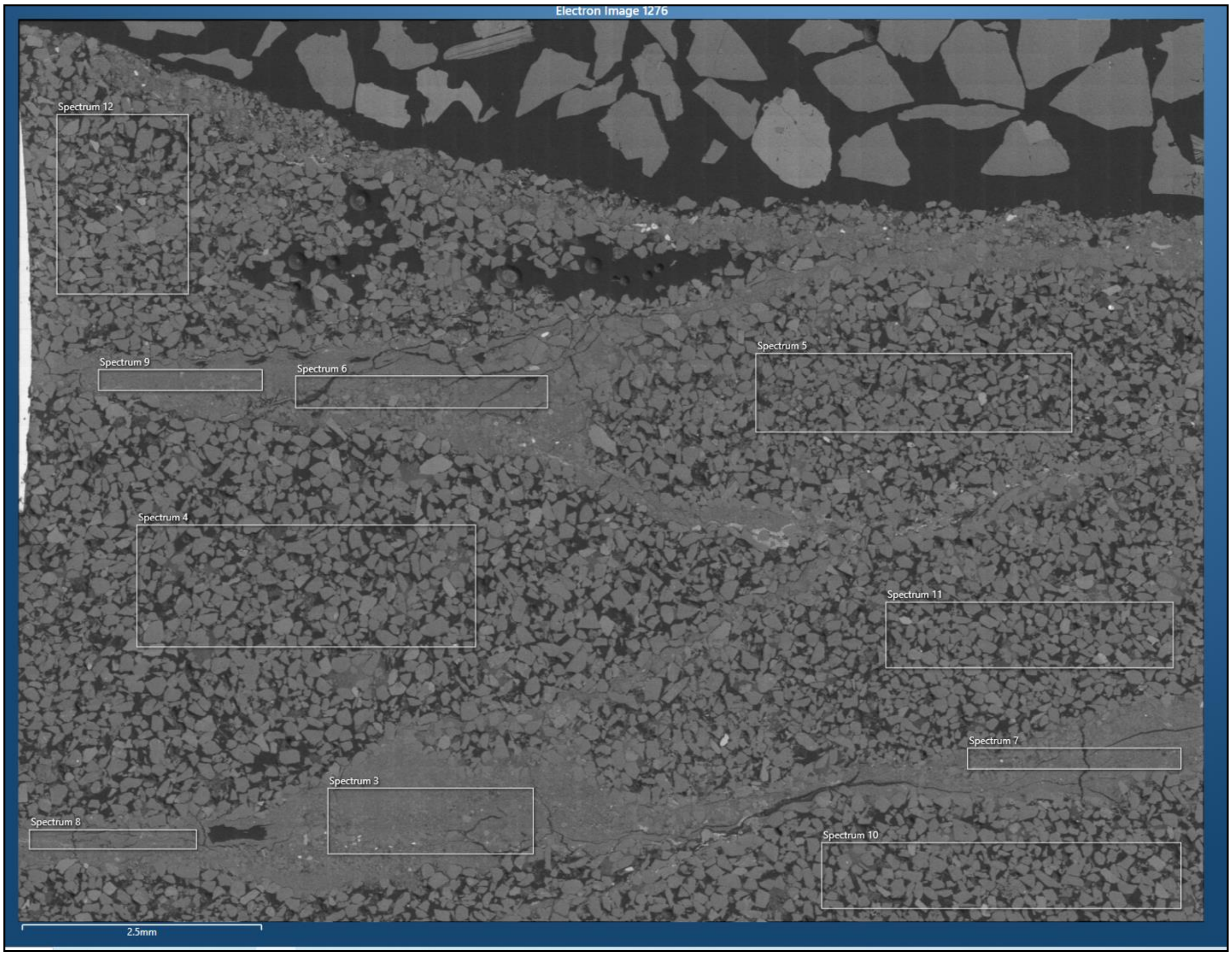

Figure S8. BSE image of the spike thin section (L9L 005 PE) with regions of interest where spectra were obtained demarcated. Note that Spectra 1-2 were test regions of interest (to help calibrate EDS parameters) and are not reported, hence why the naming within the software begins at three.

Table S1 reports the results of these averaged spectra for the fossil integument rendering layer and sand (both internal and external), bearing in mind that the areas of each ROI differ. In general, the internal and external sand is of similar composition.

Compared to the sand, the fossil has similar concentrations of Si and O, but is likely enriched in Na, Mg, Al, K, Ca, Fe. This is consistent with a aluminosilicate clay-enriched composition compared to the surrounding sand matrix. Furthermore, the presence of Fe could partly explain the dark staining present on some regions of the skin renderings of the adult hadrosaur mummy (e.g., decay-associated iron sulfides, weathering-derived iron oxides, etc.).

Furthermore, the fossil is actually depleted in C compared to the sand matrix. This pattern is possibly due to the fact that the main C signal comes from the embedding epoxy. The clay layer is smaller grained, and thereby smaller pored, than the sand matrix. This difference means that resin infiltration is limited in the fossil layer compared to the large gaps between sand grains. Regardless, the reduced C is certainly not consistent with the fossil integument renderings being preserved as organically fossilized soft tissues.

Spectrum Label	**C**	**O**	**Na**	**Mg**	**Al**	**Si**	**Cl**	**K**	**Ca**	**Ti? Ba?**	**Fe**	**Cu**	**W? Si?**	**Os**	**U**
Spectrum 3 Fossil	14.91	61.16	0.43	0.62	3.57	14.31	0.13	0.81	1.01	0.14	0.95	0	1.49	0.47	0
Spectrum 4 Internal sand	20.78	67.71	0	0	0	10.68	0.15	0.33	0.17	0.04	0.14	0	0	0	0
Spectrum 5 External sand	20.07	66.86	0.32	0.23	1.09	10.42	0.13	0.23	0.43	0	0.22	0	0	0	0
Spectrum 6 Fossil	17.09	63.89	0.37	0.51	3.07	12.69	0.11	0.67	0.76	0.1	0.74	0	0	0	0
Spectrum 7 Fossil	15.85	62.75	0.45	0.67	3.24	14.16	0.12	0.73	1.08	0.13	0.82	0	0	0	0
Spectrum 8 Fossil	15.69	62.35	0.26	0.63	3.84	13.67	0.11	0.85	0.71	0.11	1.78	0	0	0	0
Spectrum 9 Fossil	20.74	44.05	0.62	0.97	5.88	22.38	0.13	1.69	1.01	0.23	1.9	0	0	0	0.38
Spectrum 10 External sand	43.5	37.51	0	0	0	17.31	0.27	0.62	0.39	0.05	0.35	0	0	0	0
Spectrum 11 External sand	42.14	38.33	0	0	0	17.76	0.26	0.62	0.42	0.1	0.38	0	0	0	0
Spectrum 12 Internal sand	41.26	37.13	0.37	0.23	1.91	16.62	0.23	0.83	0.61	0.06	0.43	0.3	0	0	0
Fossil average (*n*=5)	16.86	58.84	0.43	0.68	3.92	15.44	0.12	0.95	0.91	0.14	1.24	0	0.3	0.09	0.08
Internal sand average (*n*=2)	31.02	52.42	0.19	0.12	0.96	13.65	0.19	0.58	0.39	0.05	0.29	0.15	0	0	0
External sand average (*n*=3)	35.24	47.57	0.11	0.08	0.36	15.16	0.22	0.49	0.41	0.05	0.32	0	0	0	0
Sand overall average (*n*=5)	33.55	49.51	0.14	0.09	0.6	14.56	0.21	0.53	0.4	0.05	0.3	0.06	0	0	0

Table S1. Elemental relative percent compositional profiles (i.e., values of the 15 auto-assigned elements by Aztec software reported sum to 100, barring rounding error) from EDS of the spectra indicated in the BSE Figure S8 (above). Averages of the fossil clay layer, internal sand grains, and external sand grains listed in the bottom rows. Internal and external sand have similar composition. Highlighted colors of cells in the first-row header indicate notable elements that appear to be either enriched in (green), similar to (blue), or depleted in (red) the fossil compared to the sand. Note that sample size, *n*, simply refers to the number of spectra averaged from the list above. Each spectrum, however, has a different area, so these averages are approximate values and not tightly controlled for the number of pixels. Due to automatic identification of the Aztec software, the assigned Ti peaks are perhaps more likely to be Ba, while assigned W peaks are more likely to be Si.

4.2. Basement scale that separated from tail spike block of early adult 'mummy' (UCRC PV30) –

When removing the spike block (Figure S1) from the tail of the early adult 'mummy' (UCRC PV30), a single basement scale separated from the block and was analyzed separately under BSE and EDS. Note that the scale was exposed to the Epotek 301 epoxy applied to the blocks surface, which can be overserved as colocalized C and Cl signatures on its surface under EDS (Figure S9).

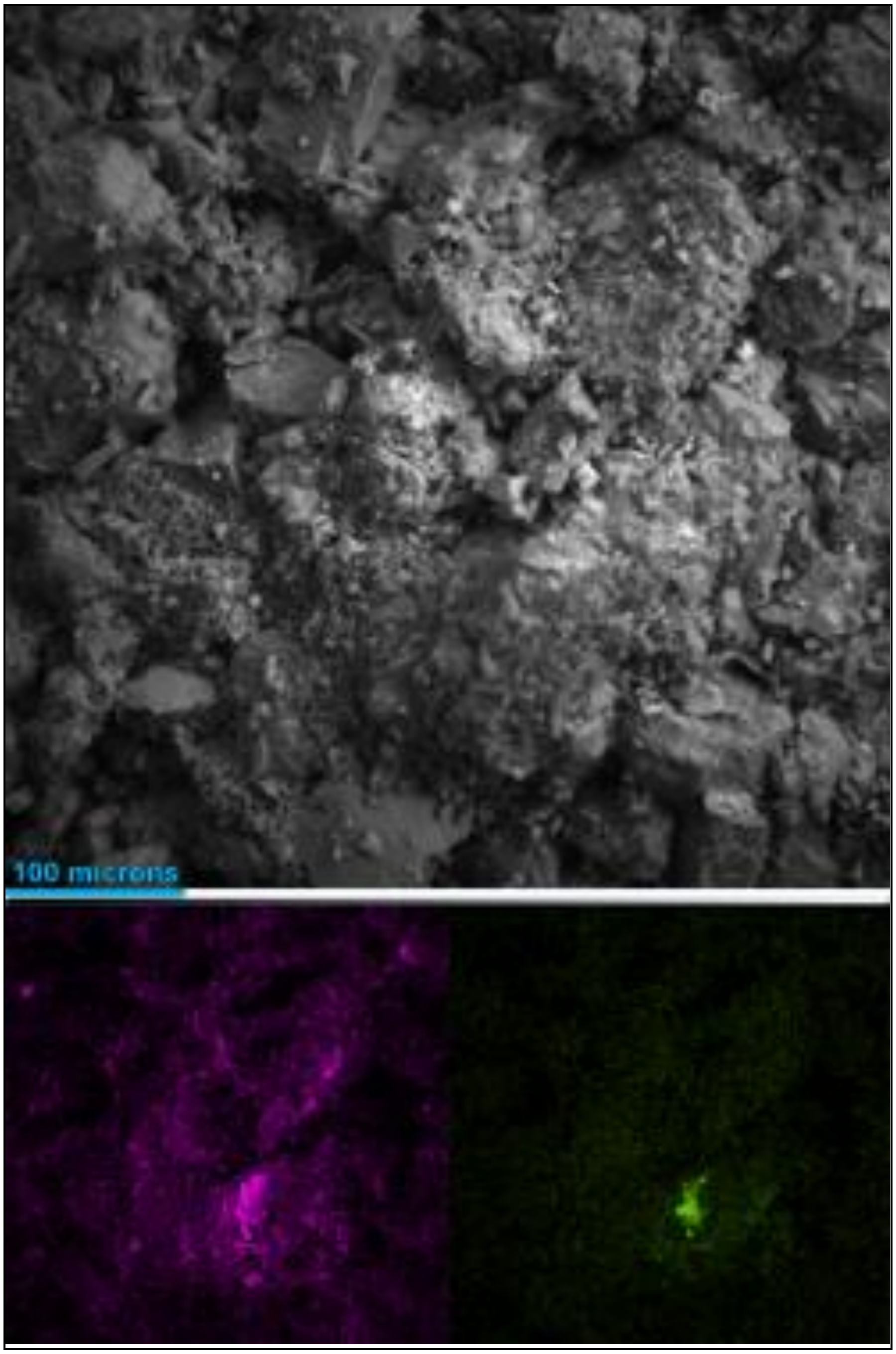

Figure S9. BSE (top), showing individual blocky sand grains obscured by a surface coating, and EDS maps (below) for C (purple) and Cl (green) on the surface of the single basement scale that separated off of the spike block from the tail of the early adult ‘mummy’ (UCRC PV30).

4.3. Late juvenile ‘mummy’ (UCRC PV31) –

The integument rendering sampled from the late juvenile *Edmontosaurus* ‘mummy’ (UCRC PV31) is relatively enriched in Ca compared to the internal sediment matrix separating it from the scapula. The Ca signal shows some colocalization with Mg, but not with P. Compare Figures S10–S11 to Figure 11.

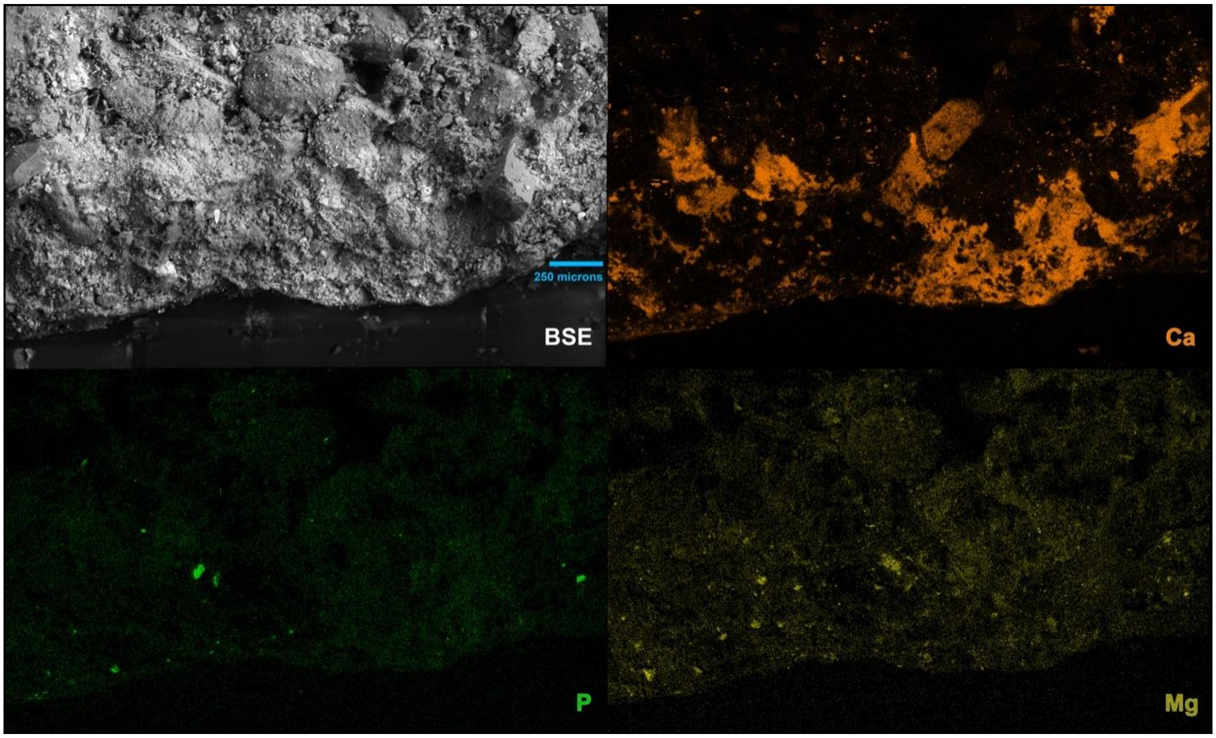

Figure S10. Late juvenile 'mummy' (UCRC PV31) sample removed from integument rendering and internal sediment above the scapula, showing large BSE and EDS maps of key elements. The sample's naturally broken cross section is facing the viewer with the sediment surface contacting the scapula towards the top (out of frame), the clay template layer toward the bottom, and the internal sediment matrix between.

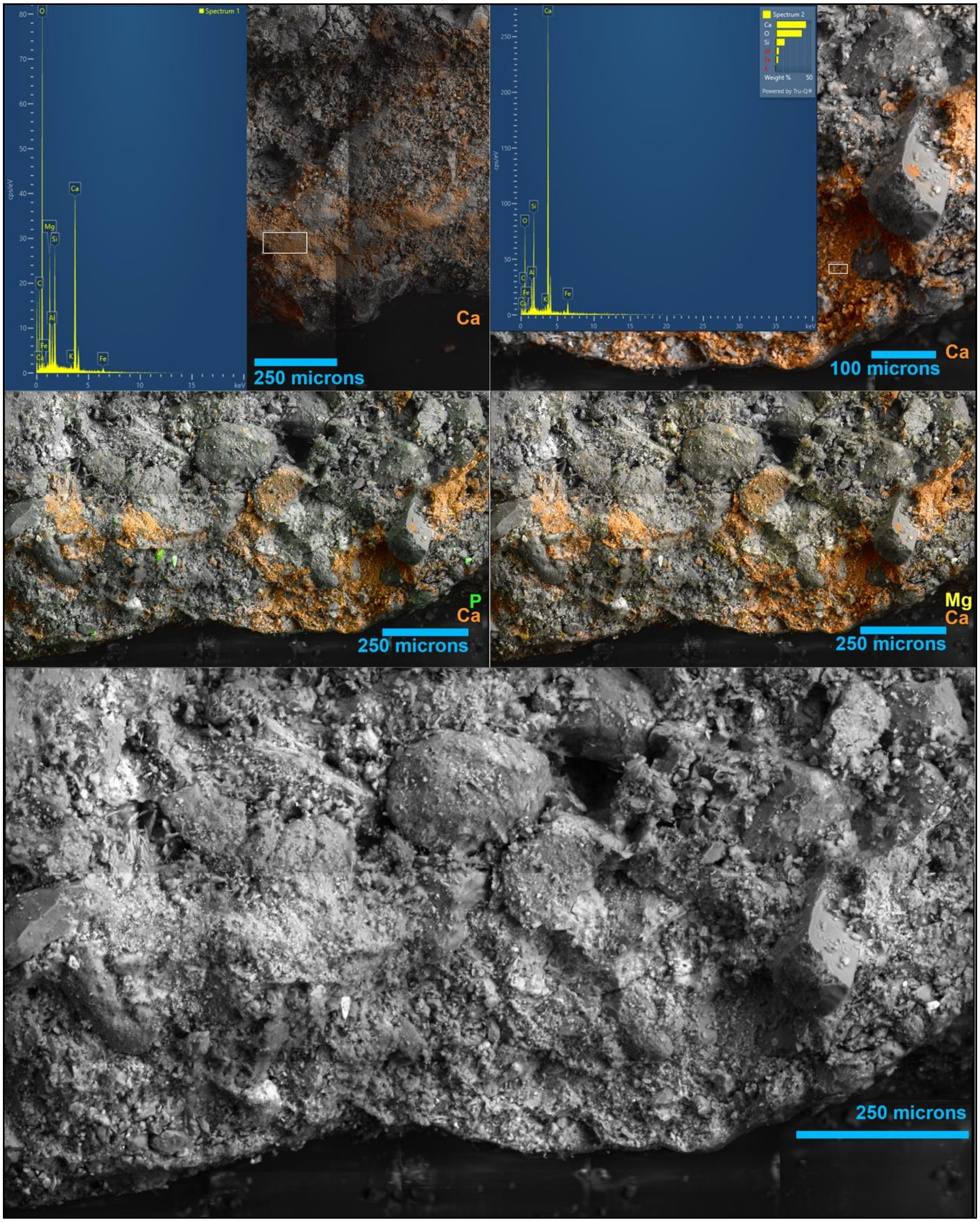

Figure S11. Late juvenile 'mummy' (UCRC PV31) sample removed from integument rendering and internal sediment above the scapula. The sample's naturally broken cross section faces the viewer with the sediment surface contacting the scapula towards the top (out of frame), the clay template layer toward the bottom, and the internal sediment matrix between. BSE, EDS spectra, and elemental maps shown. Top left EDS spectrum corresponds to the white rectangular ROI in the top left BSE image. Top right EDS spectrum corresponds to the white rectangular ROI in the top right BSE image.

4.4. Plant material under tail of early adult 'mummy' (UCRC PV30) –

Reported in Figure S12 is the EDS spectrum from the plant material under the tail (see Fig. 18) of the early adult *Edmontosaurus* 'mummy' (UCRC PV30). Note limited Cl signal by elemental weight percentage.

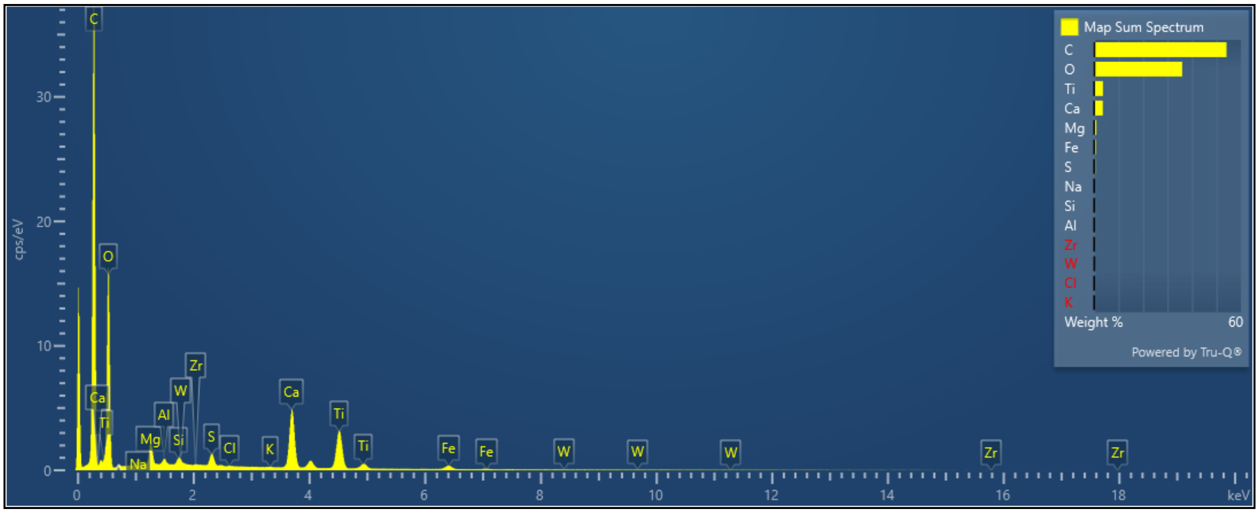

Figure S12. EDS spectrum from plant material under the tail of early adult *Edmontosaurus* 'mummy' (UCRC PV30). Note that, due to automatic identification of the Aztec software, the Ti peaks are perhaps more likely to be Ba, while W peaks are more likely to be Si.

SOM 5. Laser Ablation-Inductively Coupled Plasma-Mass Spectrometry

Although Table 4 presents all LA-ICP-MS elemental concentrations rounded to the nearest whole ppm, many elements have limits of detection below 1 ppm under our analytical equipment (Figure S13). We also present the raw LA-ICP-MS data for the minor/trace elements (including rare earth elements) as unrounded averages in Table S2. Do keep in mind, however, the varying limits of detection between different elements when examining the raw, unrounded data.

Table S2 (below). Raw LA-ICP-MS data (unrounded) for minor and trace elements from the early adult Edmontosaurus UCRC PV30 fossil spike and associated sediment matrix. Compare to rounded values in Table 4 and note the varying limits of detection between different elements as shown in Figure S13.

Minor & trace elements	Average ppm (unrounded) fossil spike flake (*n* = 10 sites)	Average ppm (unrounded) sediment (*n* = 10 sites)
Li	12.2034862	7.38607377
Be	1.89324532	3.34203622
B	31.0980145	67.5454944
Sc	10.5697036	6.94200621
Ti	2451.61853	245.246264
V	66.5637502	34.4804379
Cr	41.8581962	515.774317
Ni	108.525958	13.238933
Co	69.1645723	5.30565913
Zn	327.646062	188.995406
As	262.089845	72.6980853
Rb	79.8888336	57.2867516
Sr	103.872576	40.7595094
Zr	140.737942	36.4402724
Nb	12.8493828	8.71986824
Ag	0.44541811	3.40103835
In	0.21623142	3.41498668
Sb	5.55046524	100.322959
Cs	3.65374785	2.77218945
Ba	502.585542	280.131724
La	19.6141251	10.5782118
Ce	34.1708996	25.1236468
Pr	4.45594032	2.77717876
Ta	1.15558855	0.28502448
Au	0.02634367	0.28399769
Y	14.4798843	6.35669917
Bi	0.63101989	0.49748457
U	2.95964315	1.35030659
W	1.23103138	1.11199398
Mo	17.4969662	26.6172111
Nd	16.03401	6.9261816
Sm	3.27663958	1.02084224
Eu	0.82833276	0.42909453
Gd	2.95881626	1.45919649
Tb	0.41942372	0.16276616
Dy	2.5838448	1.04408874
Ho	0.54733544	0.48674009
Er	1.5843532	0.66568649
Tm	0.24771879	0.37063914
Yb	1.65812287	0.73459356
Lu	0.28028998	0.41368035

Hf	5.37214503	1.25959151
Th	7.81286867	4.05018994

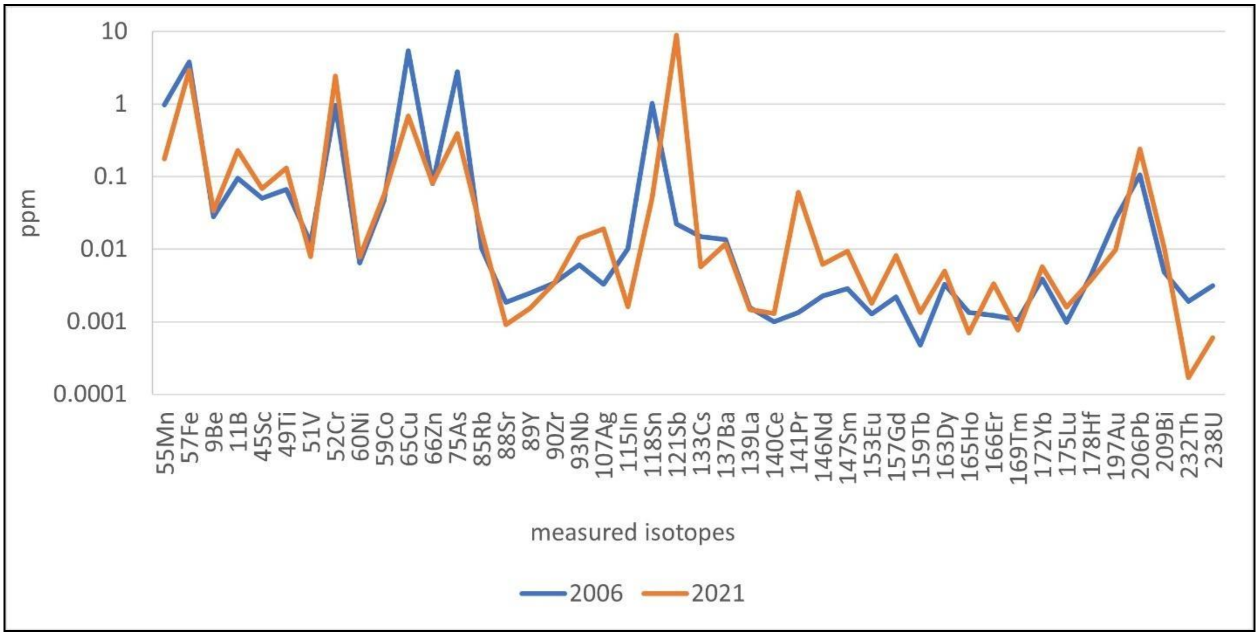

Figure S13. LA-ICP-MS limit of detection by element for the equipment at the Field Museum.

SOM 6. X-ray Diffraction & Laser-stimulated Fluorescence Photography

XRD (see Table 5) performed at the University of Illinois Urbana-Champaign Illinois State Geological Survey X-ray Diffraction Laboratory included XRD bulk analysis on the AQ (anterior quarter) 150-micron thin section (~2.54 cm diameter beam was centered on the external matrix immediately adjacent to the fossil layer) from the tail spike of the early adult *Edmontosaurus* ‘mummy’ spike (UCRC PV30). The X-ray beam location is shown on a LSF photograph of the thin section in Figure S14.

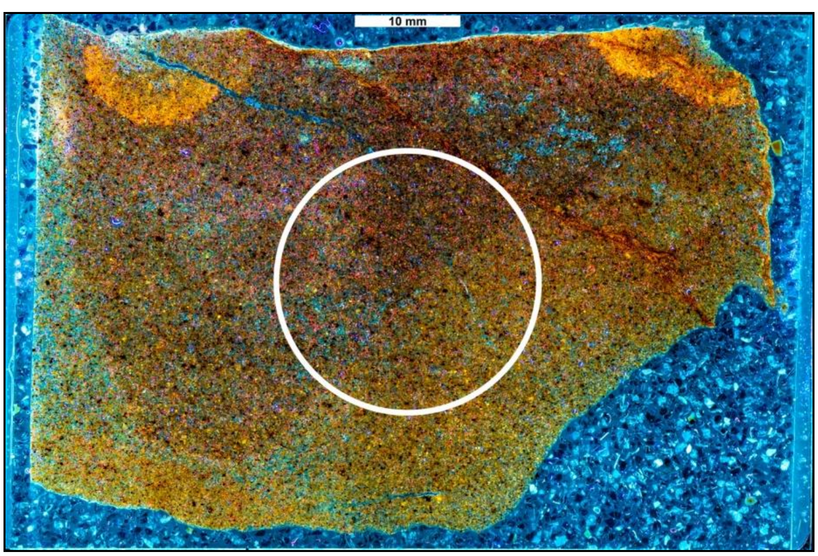

Figure S14. Approximate XRD beam position (white circle) for XRD clay analysis at the University of Illinois-Urbana Champaign of the sediment immediately adjacent to the fossil integument rendering layer (dark brown triangular cross section to the top right of the slide) shown on the LSF digital photograph of the AQ (anterior quarter) 150-micron thin section of the early adult *Edmontosaurus* spike.

SOM 7. Sedimentological Photography

Additional images of rip-up clasts on the late juvenile *Edmontosaurus* 'mummy' (UCRC PV31) are shown in Figures S15–S16.

Figure S15. Rip-up clasts below the hips of the late juvenile *Edmontosaurus* 'mummy' (UCRC PV31).

Figure S16. Rip-up clasts inside the shortest dorsal ribs on left side of the late juvenile *Edmontosaurus* 'mummy' (UCRC PV31).